Dual Mode Inspection Using Guided Waves and Phased Array Ultrasonics from a Single Transducer

Konstantinos Tzaferis[1 [0000−0001−7356−6249]], Morteza Tabatabaeipour[1 [0000−0002−9355−3813]], Gordon Dobie[1 [0000−0003−3972−5917]], Stephen G. Pierce[1 [0000−0003−0312−8766]], David Lines[1 [0000−0001−8538−2914]], Charles N. MacLeod[1], and Anthony Gachagan[1 [0000−0002−9728−4120]]

Centre for Ultrasonic Engineering, Department of Electronic and Electrical Engineering, University of Strathclyde, Glasgow G11XW, UK
konstantinos.tzaferis@strath.ac.uk

Abstract. Asset inspection of large structures such as storage tanks in the oil, gas and petrochemical industry is a challenging and time-consuming process. Compared to the state-of-the-art inspection methods of these structures using ultrasonic bulk wave phased array techniques, guided waves provide a mechanism for monitoring inaccessible areas and increasing the testing range to speed up the inspection process. Combining these two approaches, an efficient inspection scheme can be achieved. For this purpose, in this work, the possibility of exciting a single higher order guided wave mode at a low dispersion region is examined, using a conventional linear phased array on a 10 mm thick sample. An analytical model based on modal analysis is derived. Then, the time delays across each element of the array are optimally selected and a necessary condition on the pitch is provided, to enhance the purity of the desired mode. The results are promising, illustrating that single mode excitation is possible at high frequency-thickness products, greater or equal than 15 MHz·mm. Furthermore, the phased array transducer allows for dynamic mode selection capabilities; that is, feeding the appropriate excitation signals on each channel, different modes can be excited, without having to physically alter the transducer configuration.

Keywords: Guided waves · Linear array transducer · Modal analysis · Higher order mode excitation · Dynamic mode selection .

1 Introduction

The use of arrays for ultrasonic guided wave excitation is a compelling application gaining increasing interest [9, 11]. Although a lot of research has been conducted for the low frequency-thickness product region, below 10 MHz·mm [10], recent work has been performed in an effort to investigate higher order guided wave generation and propagation [4, 5, 11]. This adds some new challenges, mainly the increase of the modal density, which makes single mode excitation more difficult. Nevertheless, this can be compensated by increasing the

length of the active aperture [5, 11], which depends on the pitch and the number of active elements. The latter is usually limited by the number of the transmit channels of the array controller, while the former is a characteristic of the array, and can be optimally selected.

The aim of this work is twofold. The first objective is to excite a single guided wave mode at high frequency thickness products, above 15 MHz·mm, using a linear array. A necessary condition for single mode excitation is derived, setting an upper bound for the pitch. The second objective is to demonstrate the dual mode inspection capability. That is, to perform a rapid guided wave inspection followed by a detailed standard phased array inspection from the same transducer.

The organisation of this paper is as follows. First, an analytical expression for the energy spectrum based on modal analysis is derived in Section 2. Then, in Section 3, the linear time delays to enhance a specific mode are determined and a condition for single mode excitation is derived. In Section 4, simulation results of guided wave propagation are presented, highlighting the dynamic mode selection capability of the approach. Experimental results demonstrating the dual mode inspection approach are presented in Section 5. Finally, some key conclusions are drawn in Section 6.

2 Modal analysis formulation

Ultrasonic guided wave propagation in a homogeneous isotropic elastic body is most commonly performed in the context of semi-infinite media. In the special case of Lamb waves, the analysis is performed on an elastic layer with finite thickness and infinite length and width [1]. In this work, an alternative formulation based on modal analysis is presented. The approach has some differences, such that the layer is finite in all dimensions. As an immediate result, all energy quantities remain finite. Furthermore, the wavenumber assumes discrete real values, permitting expansion of the solution in an infinite series form. The whole analysis is performed in the real number domain, without the need to define any complex quantities. The layer is defined as a rectangular elastic body with length ℓ, thickness d and width w. The displacement field is then expressed in the following form,

$$\underline{u} = \left(u^1(x,z,t), 0, u^3(x,z,t)\right)$$

to enforce plane strain motion, where (x,z) the coordinates of a particle at equilibrium in the axial and thickness direction, respectively, with respect to a frame positioned at the centre of the middle cross section of the layer. The equations of motion for the linear elastic layer can be put in the form [9]

$$(\lambda+\mu)\nabla\left(\nabla\cdot\underline{u}\right)+\mu\nabla^2\underline{u}=\rho\ddot{\underline{u}},$$

where λ, μ are the Lamé constants and ρ is the density of the material. Next, separation of variables in space [12] and time and employing the free-free boundary conditions at the top and bottom edges of the layer determine the through

thickness profile of the modes, which can be divided to symmetric and antisymmetric [1, 9]. The exact boundary conditions at the left and right edges are irrelevant for the purposes of this work, since the generated guided wave is assumed to propagate in an area far from the left or right boundaries. Therefore, the trigonometric functions 1, $\cos(kx)$, $\sin(kx)$ with $k = n\frac{2\pi}{\ell}, n = 1, 2, ...$, which form a complete set in $L^2([-\frac{\ell}{2}, \frac{\ell}{2}])$, are selected as the displacement field in the x-direction. For example, an antisymmetric eigenfunction is given by

$$X^1(x,z) = (a_1 \sin(pz) + a_2 \sin(qz)) \cos(kx)$$
$$X^3(x,z) = (a_3 \cos(pz) + a_4 \cos(qz)) \sin(kx)$$

where

$$p^2 = \frac{\omega^2}{c_L^2} - k^2, \quad q^2 = \frac{\omega^2}{c_T^2} - k^2, \quad c_L^2 = \frac{\lambda + 2\mu}{\rho}, \quad c_T^2 = \frac{\mu}{\rho}$$

and a_1, a_2, a_3, a_4 as given in [1]. The modes in the frequency-wavenumber domain

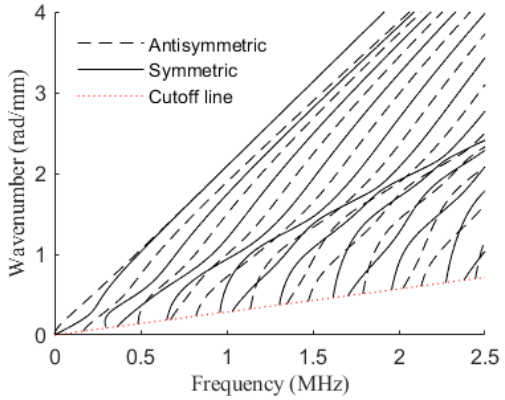

Fig. 1. Lamb wave modes (black) for a 10 mm aluminium layer in frequency-wavenumber domain and cutoff line (red).

for a 10 mm aluminium layer are shown in Figure 1. The modes are calculated using the Dispersion Calculator (DC) [3].

In a guided wave excitation study, emphasis is placed to determine the excitation parameters to focus the energy on a specific mode. Therefore, the natural object to study is the total energy (energy spectrum), which shows how the energy is distributed among different modes. The total energy of the system is the summation of the kinetic and potential energy,

$$E = T + V = \frac{1}{2}\int_V \rho \langle \dot{\underline{u}}, \dot{\underline{u}} \rangle_{\mathbb{R}^3} dV + \frac{1}{2}\int_V U dV = \dot{\tau}^i g_{ij} \dot{\tau}^j + \tau^i k_{ij} \tau^j \qquad (1)$$

where $\underline{u} = \tau^i \underline{X}_i$ is the series expansion of the total solution [2] , U is the strain energy of the layer and g_{ij} and k_{ij} are the metric [8] and stiffness tensors, respectively. Note that the summation convention on repeated indices is employed. The exact form of the energy spectrum depends on the time coefficient functions $\tau^i(t)$, which in turn depend on the excitation load $\underline{f}(x, y, t)$, and the initial conditions of the displacement and velocity fields, which are assumed to be zero. In this work, the excitation load $\underline{f}$ corresponds to an appropriately time delayed piston-like pressure load at the region of each element. The energy spectrum and the excitation spectrum that is directly derived from it are the main objects that determine all relevant parameters for single guide wave mode excitation, as is shown in the next section.

3 Guided wave excitation with a phased array

A common guided wave excitation method with a linear array transducer is to mimic the single-element coupled with a wedge set up, by steering the beam at a desired angle using linear time delays [9]. In the general case, this will create two beams in the layer, one propagating at the forward and another at the backward direction. For the purposes of this work, only the forward propagating wave is relevant. This can be justified by the presence of multiple elements, which can be used to distinguish between the forward and backward waves. Next, employing linear time delays and after simple but tedious algebraic manipulations of (1), the energy spectrum for propagation in the forward direction appears in the form [9]

$$E = E_s F_+,$$

where E_s depends solely on the response of a single element and

$$F_+(\omega, k\,; s, N, \tau) \equiv \frac{\sin^2(\frac{1}{2}N(ks - \omega\tau))}{\sin^2(\frac{1}{2}(ks - \omega\tau))} \tag{2}$$

is the excitation spectrum, which for a given frequency and wavenumber value depends only on the parameters related to the array, namely the pitch, the number of elements and the time delay law. A similar decomposition based on the normal mode expansion method is presented in [9]. To enhance a certain mode, say at (f_e, k_e), in this work, the time delay constant [11] is determined according to

$$\omega\tau = ks \Rightarrow \tau = \frac{k_e s}{2\pi f_e} = \frac{s}{V_{\text{ph}}}. \tag{3}$$

The excitation spectrum to enhance the symmetric mode $S1$ at $f_e = 1.8$ MHz for an array with pitch $s = 2$ mm and $N = 32$ elements is shown in Figure 2. The multiple excitation beams (shown in yellow in Fig. 2) are given by

$$k = \frac{k_e}{f_e} f + \frac{2\pi m}{s}, m = 0, -1, -2, ...$$

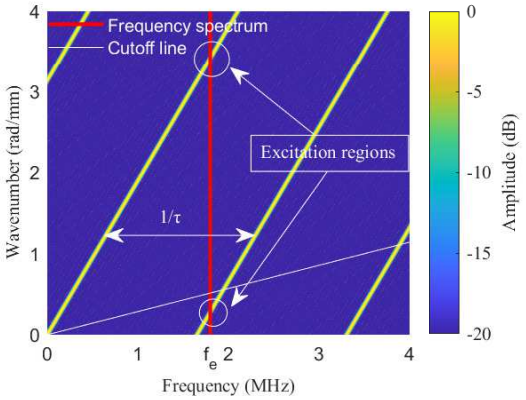

Fig. 2. Excitation spectrum for a 32 element array with pitch 2 mm. The time delays are set to 605 ns to excite $S1$ at 1.8 MHz. The first (primary) and second excitation beams are shown, separated by $1/\tau$. The red vertical line corresponds to the frequency spectrum centred at f_e. The second beam intersects with the frequency spectrum, therefore, condition (4) is violated. Nevertheless, since the intersection region is below the cutoff, the more accurate condition (5) is satisfied.

The distance between two adjacent beams is $1/\tau$. The primary beam ($m = 0$) corresponds to excitation at constant phase velocity [11]. For single mode excitation, only one excitation beam should intersect with the frequency spectrum. This necessary condition is stated as:

$$\frac{1}{\tau} > f_e \Rightarrow \frac{2\pi f_e}{k_e s} > f_e \Rightarrow \frac{2\pi}{k_e s} > 1 \Rightarrow s < \lambda_e. \tag{4}$$

A more accurate condition can be derived using the cutoff line which can be approximated as a line with constant slope, as shown again in Figure 2. Exploiting the fact that modes exist only above the cutoff line, $k > \frac{2\pi}{V_{\text{cutoff}}} f$, the condition takes the form

$$\frac{k_e}{f_e} f_e - \frac{2\pi}{s} < \frac{2\pi}{V_{\text{cutoff}}} f_e \Rightarrow s < \frac{\lambda_e}{1 - \frac{V_{\text{ph}}}{V_{\text{cutoff}}}}. \tag{5}$$

Condition (5) sets an upper bound for the pitch. This condition assumes sufficiently small excitation and frequency bandwidths, nevertheless, it is a good approximation even when this is not the case. Note that selecting a large pitch increases the length of the active aperture, which decreases the bandwidth of the spectrum [11]. For that reason, the optimal pitch selection to improve the purity of the targeted mode is a value close but lower to the right hand side of (5).

4 Simulation results

In this section, 2D numerical models using FEM based software OnScale [7] were developed. Specifically, higher order guided wave generation and propagation using a linear array with element size 0.5 mm and pitch 0.75 mm on a 10 mm aluminium plate was simulated. The action of the array was modelled using normal forces applied to the top surface at the region corresponding to active elements. To enhance a specific mode, the appropriate time delay law was determined from equation (3). The displacement component normal to the surface along a 120 mm long line with spatial sampling step 0.1 mm was monitored. The displacements were sampled at the bottom surface. This means that the Rayleigh wave is not detected, which in this case is beneficial, since in the present experimental setup only the first 32 elements of an 128 element array were excited, thus the Rayleigh wave is damped by the presence of the non active elements of the linear array. A similar result has also been reported in [5]. Two configurations, each one with different number of elements and targeted

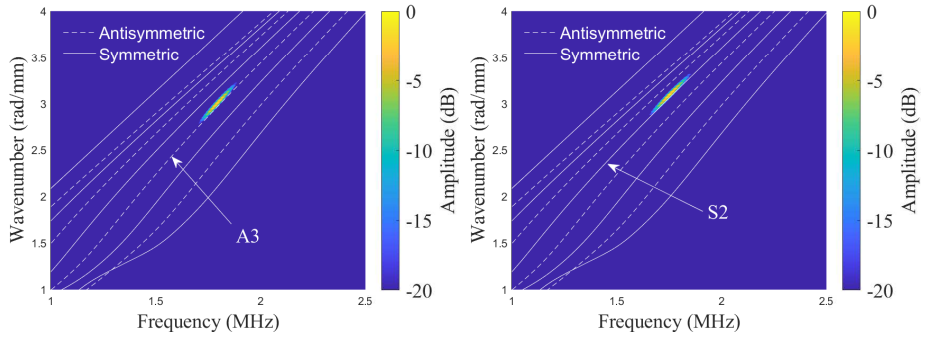

Fig. 3. 2DFFT of monitored simulation signals. Left: 32 element array using a 14-cycle Hanning windowed toneburst at 1.8 MHz. Mode $A3$ was targeted, corresponding to $\tau = 200$ ns. Right: 64 element array using a 10-cycle Hanning windowed toneburst at 1.8 MHz. A different mode, namely $S2$ was targeted using $\tau = 210$ ns, showing the dynamic mode selection capability of the approach.

modes were developed. The first consists of an array of 32 elements, excited by a 14-cycle Hanning windowed toneburst at 1.8 MHz, resulting to a 18 MHz·mm frequency-thickness product. The targeted mode was $A3$. The 2DFFT is shown in Figure 3 (left). The second configuration modelled a 64-element array excited with a 10-cycle Hanning windowed toneburst at 1.8 MHz. The time delay law was set to enhance $S2$. The 2DFFT is shown in Figure 3 (right). In both simulations, the mesh size was set to 0.1 mm and the time step was equal to 10 ns. Note that at 1.8 MHz, the wavelengths of $A3$ and $S2$ are approximately $\lambda_{A3} \approx 2.1$ mm and $\lambda_{S2} \approx 2$ mm, thus condition (5) is satisfied in both cases.

The presented simulations highlight a significant advantage of the phased array excitation. Both simulation set ups can be realised with the same array, each time controlling the parameters of the excitation electronically, thus the targeted mode can be dynamically selected [9].

5 Experimental results

5.1 Experimental 2DFFT

To validate the results presented in the above section, experiments were conducted on a 10 mm aluminium plate. More specifically, a linear 2.25 MHz Vermon array was used for the transmission of the guided wave, while an identical array recorded the u_3 displacement component. The nominal pitch of the arrays is equal to 0.75 mm. The arrays were controlled with the 32Tx/32Rx/128E FI Toolbox, a hardware that can generate arbitrary waveforms and implements the Full Raw Data [6] utility. All the excitation parameters were identical to the ones

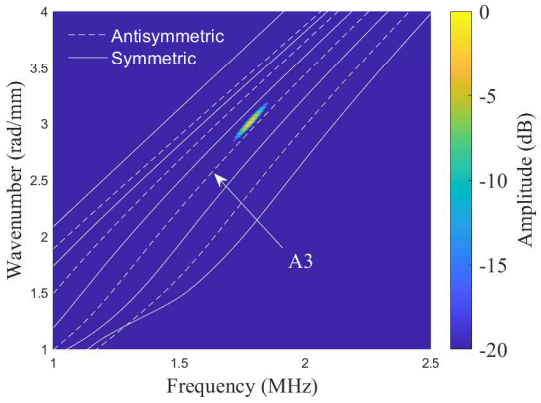

Fig. 4. Experimental 2DFFT using a 32 element active aperture and pitch 0.75 mm. Mode $A3$ was targeted. The excitation parameters were identical to the ones selected for the first simulation, see Fig. 3 (left).

selected for the first simulation. The receiver monitored data along a 120 mm long line at the top surface of the plate with a sampling step equal to the pitch of the array. The raw data were then post processed in the host PC. The 2DFFT of the acquired raw data is shown in Figure 4. Both simulation and experimental results are in excellent agreement.

5.2 Guided wave scan

The sensitivity of the excited higher order mode was tested against a machined defect that can be approximated as a flat bottom hole. The hole is 5.5 mm deep

with diameter 12 mm, as shown in Figure 5 (bottom). A linear scan in pitch-catch configuration was performed, see Figure 5 (top). The scan was performed manually, with scanning step approximately 1 mm. A simple frame was used to keep the transducers aligned and at a fixed distance (not shown in Figure 5.2), approximately 28 cm. At each step, the maximum amplitude of $A3$ was extracted. The amplitude of $A3$ versus the y'-coordinate of the centre of the

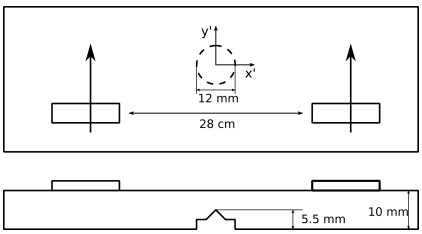

Fig. 5. Top: Schematic of the top view of a 10 mm aluminium plate. Two transducers in pitch-catch configuration were used to performed a linear scan in the direction of the arrows. Bottom: Schematic of cross section showing the geometry of the defect.

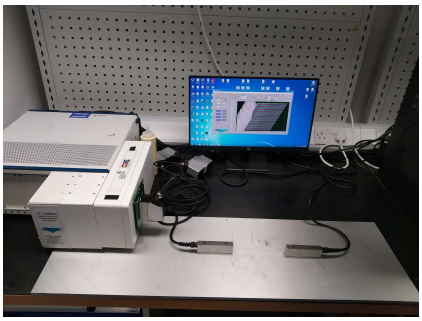

Fig. 6. Experimental set up showing the two linear arrays on top of the 1m × 30cm × 10mm aluminium plate and the array controller.

transmitter (or the receiver) with respect to a frame located at the centre of the defect, as shown in 5 (top) is plotted in Figure 7. The amplitude starts dropping

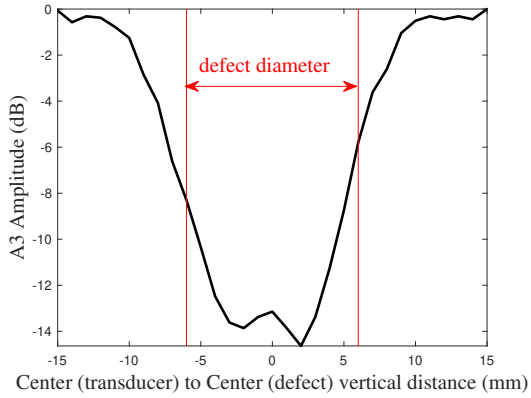

Fig. 7. Guided wave linear scan in pitch-catch configuration. The amplitude of mode $A3$ reaches the minimum when the transducers are aligned with the defect.

when the transducers enter the defect region. Since the size of the elements of the transducers are 12 mm in the scan direction and the radius of the defect is 6 mm, the transducers enter the defect region at ±12 mm. The maximum amplitude drop occurs when the the transducers are aligned with the defect, resulting to an amplitude drop of approximately −14 dB.

5.3 Phased Array Inspection

Although the defect is successfully located along a line, its exact position and size are still unknown. For that reason, a standard ultrasonic phased array inspection was performed with the same probe, to accurately position and size the defect. A linear scan was performed, using all 128 elements of the array and an active aperture of 16 elements. The B-scan of the defect region is shown in Figure 8. The back wall and defect reflections are clearly visible and marked. The dimensions of the defect were derived based on the axial length of the figure, which is $128 \cdot 0.75 = 96$ mm and the distance between the two back wall reflections, which is $2d = 20$ mm. The diameter and depth as estimated from the B-scan are successfully marked in Figure 8.

This experiment suggests it is possible to use higher order guided waves as a screening method, followed by a detailed phased array inspection from the same transducer, at least for the examined scenario. Further studies need to be conducted for a larger class of defects and guided wave modes, while more involved post-processing algorithms can improve the guided wave inspection.

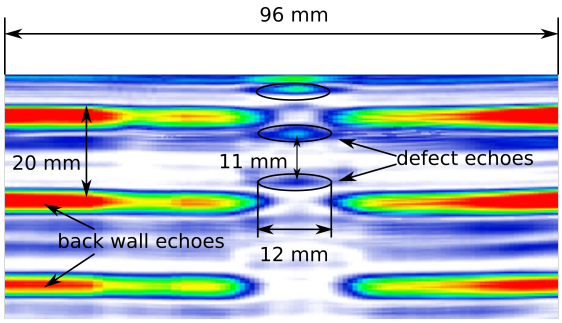

Fig. 8. Normal Phased Array Inspection. The intact and defect regions are clearly visible. The defect is successfully located and sized.

6 Conclusions

In this work, the excitation of a higher order single Lamb wave mode was studied in some detail, deriving a necessary condition for the pitch. The approach was tested under simulations, followed by experimental results. Then, a scheme

combining two different inspection modes, namely guided and bulk wave ultrasonics, was demonstrated. A flat bottom hole was successfully located using guided wave testing, and then was accurately sized using standard bulk wave phased array inspection. This was done from the same transducer, showing that it is possible to employ guided waves as a screening method and then a more detailed inspection using the same hardware.

References

1. Achenbach, J.D.: Reciprocity in elastodynamics. Cambridge University Press (2003)
2. Craig, R.R.: Structural Dynamics: An Introduction to Computer Methods. Wiley (1981)
3. Huber, A.: Dispersion Calculator (DC). `https://www.dlr.de/zlp/en/desktopdefault.aspx/tabid-14332/0A24874_read-61142/#/gallery/33485` (2018)
4. Jayaraman, C., Krishnamurthy, C.V., Balasubramaniam, K., Thompson, D.O., Chimenti, D.E.: Higher order modes cluster (homc) guided waves—a new technique for ndt inspection. pp. 121–128. AIP (2009). https://doi.org/10.1063/1.3114094
5. Khalili, P., Cawley, P.: Excitation of Single-Mode Lamb Waves at High-Frequency-Thickness Products. IEEE Transactions on Ultrasonics, Ferroelectrics, and Frequency Control **63**(2), 303–312 (feb 2016). https://doi.org/10.1109/TUFFC.2015.2507443
6. Lines, D., Wharrie, J., Hottenroth, J.: Multi-channel ultrasound toolbox: A flexible modular approach for real-time array imaging and automated inspection (2010)
7. OnScale: version 1.27. OnScale Inc., 770 Marshall Street Redwood City, CA 94063 (2019)
8. Paraskevopoulos, E., Natsiavas, S.: On application of Newton's law to mechanical systems with motion constraints. Nonlinear Dynamics **72**(1-2), 455–475 (apr 2013). https://doi.org/10.1007/s11071-012-0727-1
9. Rose, J.L.: Ultrasonic Guided Waves in Solid Media. Cambridge University Press (2014)
10. Tabatabaeipour, M., Trushkevych, O., Dobie, G., Edwards, R.S., McMillan, R., Macleod, C., O'Leary, R., Dixon, S., Gachagan, A., Pierce, S.G.: Application of ultrasonic guided waves to robotic occupancy grid mapping. Mechanical Systems and Signal Processing **163** (1 2022). https://doi.org/10.1016/j.ymssp.2021.108151
11. Veit, G., Bélanger, P.: An ultrasonic guided wave excitation method at constant phase velocity using ultrasonic phased array probes. Ultrasonics **102** (mar 2020). https://doi.org/10.1016/j.ultras.2019.106039
12. Xing, Y.F., Liu, B.: Exact solutions for the free in-plane vibrations of rectangular plates. International Journal of Mechanical Sciences **51**(3), 246–255 (2009). https://doi.org/10.1016/j.ijmecsci.2008.12.009